Journal of Materials Processing Technology 238 (2016) 383–394

Contents lists available at ScienceDirect

Journal of Materials Processing Technology

journal homepage: www.elsevier.com/locate/jmatprotec

First and third generations of advanced high-strength steels in a FeCrNiBSi system

Mohsen Askari-Paykani, Hamid Reza Shahverdi*, Reza Miresmaeili

Department of Materials Engineering, Tarbiat Modares University, P.O. Box 14115-143, Tehran, Iran

ARTICLE INFO

Article history:
Received 17 April 2016
Received in revised form 20 July 2016
Accepted 27 July 2016
Available online 28 July 2016

Keywords:
Casting
Heat treatment
Advanced high strength steel
Transformation-induced plasticity
Grain rotation
Microbands

ABSTRACT

Three different solidification routes (slow, accelerated and fast) and a two-step heat treatment process were applied to a FeCrNiBSi alloy system to introduce new candidates for advanced high-strength steels (AHSSs). The evolution of the microstructure after hot roll, heat treatment, and tensile deformation was characterized using optical and electron microscopy techniques, as well as hardness and room temperature uniaxial tensile tests. The increase in the initial strain-hardening rate (strain incompatibility of microstructure components) due to grain refinement as a consequence of fast casting cooling rate results in higher mechanical properties in fast-cooling specimens with a formability index of 18.00–37.80 GPa%. Deformation-induced precipitation in the as-rolled fast-cooling specimen and transformation-induced plasticity, microband formation, and austenite grain rotation in the heat-treated fast-cooling specimen are the main dissipation energy mechanisms. The heat-treated accelerated-cooling and slow-cooling specimens with formability index of 4.75–25.50 and 2.34–14.60 GPa%, respectively, are competitive with transformation-induced plasticity, dual-phase, and complex-phase AHSSs.

1. Introduction

AHSSs are classified into three categories based on their ultimate tensile strength (UTS) and total elongation percentage (El.%). As reported by Calcagnotto et al. (2011a,b) the first generation of AHSSs has a mainly ferritic microstructure and includes dual-phase (DP), transformation-induced plasticity (TRIP), complex phases (CP), and martensitic steels (MS). Zhao et al. (2016) and Ma et al. (2016) stated that the second generation of AHSSs includes twinning-induced plasticity (TWIP), lightweight induced plasticity (L-IP), and austenitic stainless steel (AUST SS).The second generation has an austenite-based microstructure. It is described by Aydin et al. (2013) that the first- and second-generation AHSSs have UTS ranges of 500–1600 and 900–1600 MPa and El.% ranges of 5–30% and 45–70%, respectively. First-generation AHSSs were developed to extend the strength range of traditional high-strength steels beyond the 800 MPa limit. However, the increase in strength came at the expense of ductility. Demeri (2013) reported that the ductility problem was overcome with the development of austenitic second-generation AHSSs. Both generations have high UTS and excellent El.%, but they contain a high percentage of expensive alloying elements that result in higher costs and limited applications. Aydin et al. (2013) outlined that, the third-generation AHSSs are being developed in a manner that is less expensive but still provides a combination of good UTS and El.%, in ranges of 500–1600 MPa and 25–50%, respectively.

Based on the rule of mixing, Matlock and Speer (2009) proposed that the third-generation AHSSs must contain a microstructure of ferrite and martensite, with a significant amount of metastable or retained austenite above that of TRIP AHSSs. Recently, Sohn et al. (2015) developed ultra-high-strength (ferrite + austenite), duplex, lightweight steels by varying the annealing temperature of a Fe–0.7C–12Mn–5.5Al (wt.%) steel, which displayed a UTS above 1 GPa and an El.% of 46%. None of the developed steels showed a TRIP effect, and the improved tensile properties were associated with typical planar glide configurations and high dislocation-density walls, configuring Taylor lattices developed by very fine dislocation structures spaced with intervals of 50–100 nm. Deformation twinning displaying an extremely small (about 5 nm) thickness and spacing was also activated, thus resulting in additionally enhanced ductility. In developing a Fe-C-Mn-Al alloy system, Sohn et al. (2014) also presented a new ferrite–austenite duplex lightweight steel containing a low-density element, Al (Fe–0.3C–8.5Mn–5.6Al–(<0.02)(P + S) (wt.%)), which exhibited tensile elongation up to 77% and high tensile strength (734 MPa). The enhanced properties were attributed to the

* Corresponding author.
E-mail address: shahverdi@modares.ac.ir (H.R. Shahverdi).

http://dx.doi.org/10.1016/j.jmatprotec.2016.07.043
0924-0136/

simultaneous formation of deformation-induced martensites and deformation twins. In seeking an optimal design of high-carbon (0.71 wt.%), bainitic–austenitic, transformation-induced plasticity steels, Seol et al. (2012) investigated the influences of austempering temperature, chemical composition (especially the Si:Al ratio), and partitioning on the nanostructure and mechanical behavior of these steels, using atom probe tomography. They reported that reducing the Si:Al ratio from 3:1 to 1:3 caused the yield stress (Y.S.) and El.% to increase from 706 MPa and 41% to 772 MPa and 49% (austempering at 400 °C), respectively, whereas the UTS decreased from 1191 to 973 MPa. Gao et al. (2014) applied three heat-treatment routes incorporating bainite formation—bainite-based quenching plus tempering, bainite austempering, and bainite-based quenching plus partitioning (BQ&P)—to a new medium-carbon Mn–Si–Cr alloyed steel. An optimum combination of strength, ductility, and toughness was achieved after the BQ&P treatment (UTS = 1688 MPa; El.% = 25.2%; and U-notch impact toughness at 40 °C = 48 Jcm^{-2}). The enhanced mechanical properties were attributed to an increased amount of refined filmy retained austenite (22 vol.%; nanometer width range <100 nm; and submicron width range, 100–500 nm). Gutierrez-Urrutia and Raabe (2013) investigated the effect of Al content on the mechanical properties of a Fe–30.5Mn–2.1Al–1.2C (2Al) steel and a Fe–30.5Mn–8.0Al–1.2C (wt.%) (8Al) steel under different annealing conditions. The 8Al steel exhibited a UTS of 1180 MPa and El.% of 37% for a long annealing time (24 h) at 600 °C. The superior mechanical properties of the 8Al alloy were explained in terms of the precipitation of shearable nanosized κ-carbides and their role in the development of planar dislocation substructures.

In order to increase strength without compromising ductility, a FeCrNiBSi AHSS was introduced for the automotive industry, based on grain size, solid solution, and precipitation-strengthening mechanisms. As reported previously by Calcagnotto et al. (2011a,b), a high initial strain rate produced as a result of the strain incompatibility between a soft matrix and a hard second phase can improve both strength and ductility. As such, the decision was made to have an austenitic–ferritic microstructure (soft matrix) (using the Schaeffler diagram to predict the nature of the matrix) dispersed with phases of M_2B (hard second phase). Because boride precipitation can take place during solidification, it was decided that the effects of casting cooling rate on matrix grain size and boride phases would also be investigated. Cr, Ni, and Si were used to obtain an austenitic–ferritic matrix and for solid solution strengthening. As the objective of the current work was to develop a microstructure of a soft matrix and second hard M_2B phases, boron was added as a precipitation-strengthening element to increase the number of phases per unit volume. As a precipitation-strengthening role was considered for boron, the added amount was also decided to be higher than that of boron micro-alloyed steels. Three casting cooling routes were adopted to optimize the comprehensive mechanical properties. Since twin roll casting technique, in which the cooling rate can be as high as 1000 °C/S (Li, 1995), is being used to produce sheet steel products (Castrip®, 2016), it was also decided to use water-cooled Cu mold technique as one of the solidification processes. Therefore, in an attempt to respond to the demands of the automotive industry, in the current work, the effects of casting cooling rate and heat treatment process on the mechanical properties of a novel AHSS (FeCrNiBSi alloy system: AM2B®) were investigated through room-temperature uniaxial tensile and hardness tests. Furthermore, the microstructural evolution was studied systematically and the fracture mechanisms were analyzed via fractography. The UTS and El.% properties of the developed first- and third-generation AHSSs were also compared with those of other reported AHSSs.

2. Materials and methods

2.1. Casting, rolling, and heat treatment

The non-stainless multi-component master alloy in the $Fe_{59.0}Cr_{15.0}Ni_{11.5}B_{9.2}Si_{5.3}$ (at.%) [$Fe_{65.4}Cr_{15.5}Ni_{14.1}B_{2.0}Si_{3.0}$ (wt.%)] alloy system (AM2B®) was induction-melted in an alumina crucible under 10^{-4} mbar vacuum to reduce the oxidation of the master alloy. The master alloy ingot was obtained using Fe-B (containing 12 wt.% B) pre-alloy and commercially pure elements such as Fe, Cr, Ni, and Si (all 99.9% purity). Using three different solidification routes, $50 \times 50 \times 5$ mm^3 specimens were produced. The different solidification rates were obtained using an alumina mold (slow cooling (SC), ~30 °C/S), H13 mold (accelerated cooling (AC), ~ 500 °C/S), and water-cooled Cu mold (fast cooling (FC), ~1000 °C/S). To reduce excessive oxidation of the melt, a pressure vacuum caster machine was used. Resembling to twin roll casting process (Castrip®, 2016), the as-cast specimens were hot rolled for multiple passes for a total reduction of 80% (hot rolled from a thickness of 5 mm to a thickness of 1 mm). Prior to the hot rolling, the specimens were held at 1100 °C for two hours, removed from the furnace, and hot rolled before their temperature fell below 950 °C. Finally, they were allowed to cool in air. The as-rolled specimens were subjected to three different heat treatment steps. In the first heat treatment process, the as-rolled specimens were isothermally heated to 1100 °C and held for two hours (first step of route A; Fig. 1). In the second heat treatment process, the first step heat-treated specimens were given an additional isothermal heat treatment at 700 °C for 20 min (second step of route A; Fig. 1). In the third heat treatment process, the as-rolled specimens were heated to 700 °C and held for 20 min (route B; Fig. 1). The heat treatment temperatures of 1100 °C and 700 °C were chosen based on annealing temperature for AHSSs and coiling temperature of AHSS sheets, respectively (Demeri, 2013). The specimens were heated in a cast-iron filings medium in a muffle furnace. The temperature of the furnace was controlled to an accuracy of ±5 °C. The heating rate was 10 °C/min and the cooling medium was air. All further experiments were carried out with these as-rolled and

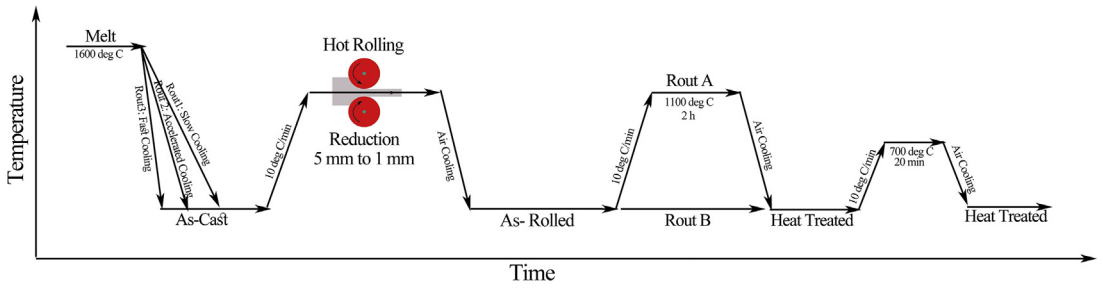

Fig. 1. Schematic of experimental procedure: three different casting cooling routs, thermo-mechanical and heat treating processes.